

# Debris-flow deposition: Effects of pore-fluid pressure and friction concentrated at flow margins

Jon J. Major\*

Richard M. Iverson

U.S. Geological Survey, 5400 MacArthur Boulevard, Vancouver, Washington 98661

## ABSTRACT

Measurements of pore-fluid pressure and total bed-normal stress at the base of several ~10 m<sup>3</sup> experimental debris flows provide new insight into the process of debris-flow deposition. Pore-fluid pressures nearly sufficient to cause liquefaction were developed and maintained during flow mobilization and acceleration, persisted in debris-flow interiors during flow deceleration and deposition, and dissipated significantly only during postdepositional sediment consolidation. In contrast, leading edges of debris flows exhibited little or no positive pore-fluid pressure. Deposition therefore resulted from grain-contact friction and bed friction concentrated at flow margins. This finding contradicts models that invoke widespread decay of excess pore-fluid pressure, uniform viscoplastic yield strength, or pervasive grain-collision stresses to explain debris-flow deposition. Furthermore, the finding demonstrates that deposit thickness cannot be used to infer the strength of flowing debris.

## INTRODUCTION

Debris flows consist of concentrated mixtures of poorly sorted sediment and water that can flow like liquids yet can stop on sloping surfaces and form nearly rigid deposits. Debris flows constitute a significant natural hazard that can cause fatalities, damage structures, and diminish land productivity. Modern debris-flow deposits line numerous mountain channels (e.g., Fryxell and Horberg, 1943; Sharp and Nobles, 1953; Curry, 1966; Broscoe and Thomson, 1969; Costa and Jarrett, 1981; Pierson, 1986; Webb et al., 1988; Nieuwenhuijzen and van Steijn, 1990; DeGraff, 1994) and blanket many subaerial and subaqueous fans (e.g., Blackwelder, 1928; Beaty, 1974; Suwa and Okuda, 1983; Hubert and Filipov, 1989; Whipple and Dunne, 1992; Masson et al., 1993; Harris and Gustafson, 1993; Blair and McPherson, 1994; Laberg and Vorren, 1995; Gori and Burton, 1996; Punongbayan et al., 1996). Ancient debris-flow deposits form distinctive strata in many sedimentary sequences (e.g., Schminke, 1967; Nemeč and Steel, 1984; Scott, 1988; Tanner and Hubert, 1991; Kim et al., 1995). Despite widespread recognition of the unique features of debris-flow deposits, the value of mechanistic interpretations of the depositional process has remained dubious. Few replicable data have been available to test hypotheses about deposition by debris flows that contain grains that commonly range in size from micrometers to meters.

Most mechanistic models of debris-flow deposition have been inspired by field observations of deposits and by small-scale laboratory experiments. For example, on the basis of deposit geometries and small-scale

experiments with clay-silt slurries, some have proposed that debris flows behave as Bingham viscoplastic materials having uniform intrinsic shear strengths and that deposition occurs if the intrinsic shear strength exceeds the gravitational driving stress (e.g., Yano and Daido, 1965; Johnson, 1970, 1984; Middleton and Hampton, 1976; Coussot and Proust, 1996). This model has served as the basis of many interpretive studies of debris-flow rheology and debris-flow deposits (Fink et al., 1981; Costa and Jarrett, 1981; Pierson, 1980; Major and Voight, 1986; Rodolfo et al., 1989; Whipple and Dunne, 1992; Blair and McPherson, 1994; Kim et al., 1995; Schwab et al., 1996). Others (e.g., Takahashi, 1978, 1991; Lowe, 1976; Vallejo, 1979) have assumed that debris flows behave as collisional grain flows of the type first analyzed by Bagnold (1954). The Bagnold model predicts that deposition occurs if resistance due to grain-collision stresses surpasses gravitational driving stress. Still other researchers have regarded debris flows as liquefied Coulomb materials (e.g., Terzaghi, 1956; Youd, 1973; Hutchinson, 1986). Youd (1973) considered debris flows to be liquefied masses that came to rest when viscous resistance exceeded driving forces, whereas Terzaghi (1956) and Hutchinson (1986) proposed that deposition resulted from pervasive decay of pore-fluid pressure, which caused Coulomb frictional resistance to increase until it overcame driving forces. Support for the various hypotheses has been largely anecdotal, however; no data from real-time field measurements or from experiments using realistic mixtures of poorly sorted debris have convincingly bolstered these hypotheses.

In this paper we present data from replicable, large-scale flume experiments that provide a new view of debris-flow motion and deposition (cf. Iverson and LaHusen, 1993a; Iverson, 1997a, 1997b; Major, 1997). The data demonstrate that debris flows can deposit poorly sorted sediment even while high pore-fluid pressure produces near-zero strength (i.e., liquefaction) in most of the mixture. Deposition of liquefied debris occurs because debris-flow movement is impeded by grain-contact friction and bed friction concentrated at surge margins where sediment is coarsest and high pore pressure is absent. Although sediment at surge margins locks frictionally during deposition, debris-flow interiors remain very weak until high pore pressure dissipates during postdepositional consolidation.

The notion that pore-fluid pressure influences the strength of a sediment-water mixture is by no means novel. Its origins are rooted in the effective-stress principle of soil mechanics (Terzaghi, 1923, 1943) and in the proposal that a soil-water mixture may deform continuously with relatively low resistance if high porosities are maintained (Casagrande, 1936). Researchers have noted that high pore-fluid pressure dissipates slowly in quasi-static debris slurries and have suggested that such pressure may influence debris-flow mobility (Hampton, 1979; Pierson, 1981; Major et al., 1997; Major, in press). Many have noted that margins of fresh debris-flow deposits are firm and afford secure footing but that deposit inte-

\*E-mail: jjmajor@usgs.gov.



**Figure 1.** Experimental debris flow descending U.S. Geological Survey debris-flow flume. Several surge waves (arrows) develop as flow descends flume. An instrumentation port (white dot) on the channel bed is located below the depth sensor suspended over the lower part of the channel. A similar instrumentation port is located in the runout area beyond the flume mouth (cf. Fig. 3). Positions of sensors within these ports are shown in Figure 4A.

riors remain too weak to walk on for days to weeks (e.g., Fryxell and Horberg, 1943; Curry, 1966; Broscoe and Thomson, 1969).

Observers of moving debris flows have provided descriptions that give the impression that flow resistance is strongly concentrated at surge fronts where coarse clasts are abundant, as if the coarse snout acted as a moving dam that impeded the movement of more-fluid debris (Rickmers, 1913; Blackwelder, 1928; Singewald, 1928; Jahns, 1949; Sharp and Nobles, 1953; Curry, 1966; Johnson, 1970; Morton and Campbell, 1974; Okuda et al., 1980, 1981; Pierson, 1986; Costa and Williams, 1984). Singewald (1928, p. 482), for example, observed that

The flowing material consisted of a black, pasty mud, which carried with it blocks and pieces of sandstone that it had engulfed along its course. Its flow was not continuous, but came in intermittent waves.... The mode of motion of the wave suggested the accumulation of material at some higher point until the resistance of the viscous material in front was overcome. In this way the resisting material was both overflowed and pushed ahead by the advancing wave.

Similarly, Sharp and Nobles (1953, p. 551) noted that

A bouldery embankment formed at the front of more viscous surges, and boulders therein rolled, twisted, and shifted about but for the most part did not appear to be rolled under. Instead, they were pushed along by the finer, more fluid debris impounded behind the bouldery dam....

Despite growing quantitative evidence of the importance of pore-fluid pressure in debris flows (Iverson and LaHusen, 1989; Eckersley, 1990; Takahashi, 1991; Iverson and LaHusen, 1993b; Iverson et al., 1997), two key factors have impeded use of this information in assessments of debris-flow deposition. First, until recently (Iverson, 1997a, 1997b), no coherent theoretical framework existed in which pore-fluid pressure was assumed to play a key role as a mediator of debris-flow friction. According to Iverson's (1997a, 1997b) theory, debris flows behave primarily as Coulomb grain flows in which intergranular friction is affected by the variable pressure of pore water containing suspended fine sediment. Second, replicable measurements that reveal the distribution of pore-fluid pressure in space and time during debris-flow deposition have not been available. In this paper, we describe such measurements and interpret them in the context of Iverson's (1997a, 1997b) theory.

## EXPERIMENTAL DEBRIS FLOWS AND DEPOSITS

We generated experimental debris flows of about 10 m<sup>3</sup> volume at the U.S. Geological Survey (USGS) debris-flow flume, a steep concrete channel 95 m long, 2 m wide, and 1.2 m deep (Iverson et al., 1992; Iverson and LaHusen, 1993a) (Fig. 1). The channel slopes 31° along its upper 88 m and gradually flattens over the lower 7 m to adjoin a concrete runout surface that slopes 3°. The sediment used in these experiments (Fig. 2; Table 1) consisted chiefly of water-saturated sandy gravel, muddy sandy gravel, and gravelly sand (Folk, 1984) containing 1–10 wt% mud (silt plus clay). Maximum particle size was generally 30 mm, but in some experiments was as large as 150 mm. For simplicity, we refer to flows containing less than 2% mud as sandy-gravel flows, and those containing about 2% to 10% mud as loamy-gravel flows, regardless of the ratio of sand to mud or the percentage of gravel.

To create a debris flow, sediment was loaded behind a steel gate at the head of the flume, soaked with water, and abruptly released. Ensuing debris flows elongated and thinned as they moved rapidly (at ~10 m/s) downslope (Iverson and LaHusen, 1993a; Iverson, 1997a, 1997b). Flows typically developed a bulbous head containing a concentration of the coarsest particles followed by a gradually tapering, finer-grained body. Moreover, multiple waves arose spontaneously and surged down the channel (Fig. 1). Each surge exhibited a conspicuous head and tail (Iverson, 1997a). Larger, faster waves overtook and coalesced with slower waves to develop even more pronounced head-and-tail morphology. Wave fronts typically developed maximum depths of 10 to 30 cm, speeds of about 10 to 12 m/s, and average periods of about 1 s (Iverson et al., 1994; Schonfeld, 1996; Iverson, 1997a). The head-and-tail morphology of the experimental flows, the concentration of coarse debris along flow margins, and the development of multiple surges mimic characteristics of natural debris flows (e.g., Blackwelder, 1928; Jahns, 1949; Sharp and Nobles, 1953; Curry, 1966; Broscoe and Thomson, 1969; Johnson, 1970; Morton and Campbell, 1974; Wasson, 1978; Okuda et al., 1980; Pierson, 1980, 1981, 1986; Costa and Williams, 1984; Takahashi, 1991).

The experimental flows decelerated rapidly and deposited sediment beyond the flume mouth on the concrete runout surface (Fig. 3). Unconfined flows traveled and deposited sediment as much as 17 m beyond the flume; flows confined by concrete panels that extended the channel length across the runout surface traveled as much as 13 m farther. Resulting deposits were

elongated and less than 40 cm thick; they covered areas of 20–80 m<sup>2</sup> (Major, 1997). The deposits exhibited morphologic and sedimentologic features common to natural debris-flow deposits, such as lobate snouts, blunt margins, marginal levees, arcuate surface ridges, clusters and streaks of accumulated surface gravel, and preferentially aligned particles along surge perimeters (Major, 1997, 1998).

Gravel commonly accumulated at surge fronts. This accumulation resulted from sorting processes during loading and flow. Gravel distribution in the deposits depended on the depositional process as well as on sorting within surge fronts. During loading of debris at the head of the flume, a reasonably homogeneous mixture was maintained, but scattered lenses of relatively well-sorted gravel sometimes formed, especially toward the front and along the sidewalls of the hopper. Videotape recordings of the gate release show that failure of the source debris involved a combination of toppling and sliding that helped mix the debris. Generally, the top of the face of the suddenly released debris toppled forward as the base of the face began to slide down the channel. Then, as the bulk of the debris advanced down the channel, adjacent debris from along the sidewalls poured through the opening. Such toppling and sliding as well as movement of debris toward the channel center rapidly sorted debris at the head of a flow, probably by a variety of processes (cf. Suwa, 1988). When flows reached the lower part of the flume, their leading edges consisted of relatively well-sorted coarse gravel followed by obviously wetter, more poorly sorted slurry (cf. Fig. 3A). Videotape recordings revealed that surge waves passing the instrumentation port in the lower flume (cf. Fig. 1) appeared coarsest at their snouts. Therefore, substantial grain-size segregation occurred within a few tens of meters of travel. In the runout area, surges deposited successive layers of sediment as they swept across or partly displaced deposits of previous waves (Fig. 3). Coarse debris at the front of many surges was commonly enveloped into the sediment deposited in lateral margins as waves decelerated and debris was shouldered aside by trailing flow (Fig. 3).

The sedimentologic character of the surge waves was evident in the sedimentary characteristics of deposits (cf. Major, 1997). Near deposit margins, relatively well-sorted gravel transported at the leading edges of flows was in

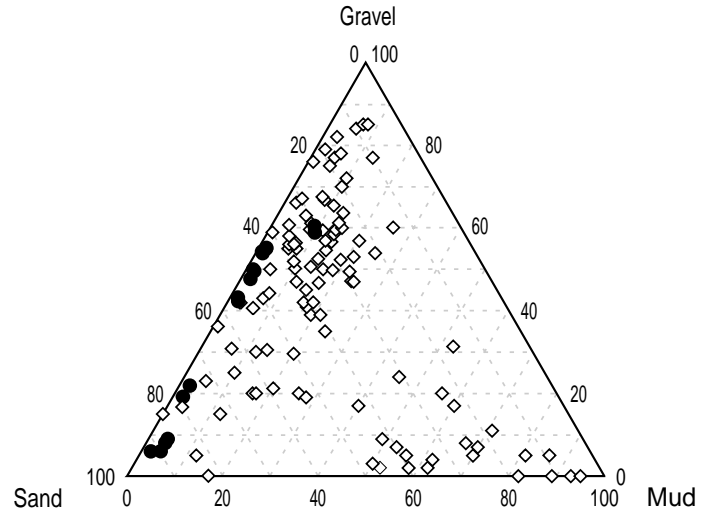


**Figure 2. Grain-size compositions of debris-flow deposits. Dots denote debris used at the U.S. Geological Survey flume; diamonds denote published analyses of natural debris-flow deposits. However, natural debris-flow deposits generally contain abundant clasts  $\geq 32$  mm in average dimension, and those grain sizes are inconsistently sampled and poorly represented in most grain-size analyses. The data in this figure are from a mixed population of samples. Some samples were restricted to grain sizes of  $\leq 32$  mm in average dimension, whereas others included clasts as large as 1 m. Nevertheless, these data show that many debris flows contain abundant coarse debris and that experiments that involve dominantly mud (silt + clay) poorly simulate most debris flows.**

TABLE 1. GRAIN-SIZE CHARACTERISTICS OF SEDIMENTS USED IN EXPERIMENTS AT USGS DEBRIS-FLOW FLUME

Debris type	Experiment number	Median grain diameter* (mm)	Mean grain diameter (mm)	Sorting coefficient (phi units)	Skewness coefficient (phi units)	Gravel (wt%)	Sand (wt%)	Silt (wt%)	Clay (wt%)
Sandy gravel	040793 <sup>†</sup>	4.2	2.9	2.3	0.3	60.6	38	1.4 <sup>§</sup>	—
		7.4	3.7	2.4	0.5	63.3	35.6	1.1 <sup>§</sup>	—
	040893 <sup>†</sup>	3.9	2.6	2.3	0.3	57.6	40.6	1.8 <sup>§</sup>	—
		5.3	3.2	2.3	0.4	64.6	33.8	1.6 <sup>§</sup>	—
	082897	5.2	3.1	2.3	0.4	62.8	35.6	1.6 <sup>§</sup>	—
		6.8	3.6	2.3	0.5	66.2	32.3	1.5 <sup>§</sup>	—
Loamy gravel	052694	5.0	3.3	2.5	0.3	61.6	37	1.4 <sup>§</sup>	—
		4.3	2.9	2.4	0.3	59.4	39.5	1.1 <sup>§</sup>	—
	083194	0.4	0.5	1.5	-0.3	13.5	84.4	1.9	0.2
		0.3	0.4	1.8	-0.3	12.8	83.3	3.6	0.3
		0.4	0.6	2.1	-0.3	19.6	76.1	3.9	0.4
	091395	0.4	0.6	2.0	-0.3	19.2	76.7	3.7	0.4
		2.3	2.5	2.6	0.0	51.8	46.6	1.5	0.1
		8.1	4.3	2.5	0.5	61.8	36.8	1.2	0.2
	090198	3.1	2.7	2.7	0.1	54.2	43.8	1.8	0.2
		1.6	2	2.8	0.0	48	49.9	1.9	0.2
		5.4	2.9	3.3	0.5	59	31.2	8.8	1.0
	090198	7.6	3.5	3.1	0.6	60.5	30.5	8.3	0.7
8.2		3.8	2.5	0.6	68.9	27.4	3.7 <sup>§</sup>	—	
	5.6	3.2	2.5	0.4	63.4	33.2	3.4 <sup>§</sup>	—	
	10.4	6.5	1.9	0.6	82.2	16.1	1.7 <sup>§</sup>	—	

Notes: Permeabilities and porosities of experimental debris were obtained from modified compaction permeameter and triaxial cell tests (see Major et al., 1997). Maximum and minimum measured values of permeability of the sandy gravel were  $5 \times 10^{-10}$  m<sup>2</sup> and  $2 \times 10^{-12}$  m<sup>2</sup>. Kindred values for the loamy gravel were  $4 \times 10^{-11}$  m<sup>2</sup> and  $4 \times 10^{-12}$  m<sup>2</sup>. Maximum and minimum measured values of porosity of the sandy gravel were 0.37 and 0.26. Kindred values for the loamy gravel were 0.41 and 0.34.

\*Median grain diameter calculated after Inman (1952); mean grain diameter, sorting coefficient, and skewness coefficient calculated after Folk (1984).

<sup>†</sup>Pore-fluid pressures were not measured in these experiments. However, the sandy gravel used as source debris in these experiments was similar to that used in experiments 041994 and 072495 in which pore-fluid pressures were measured.

<sup>§</sup>Weight percent of silt and clay combined.

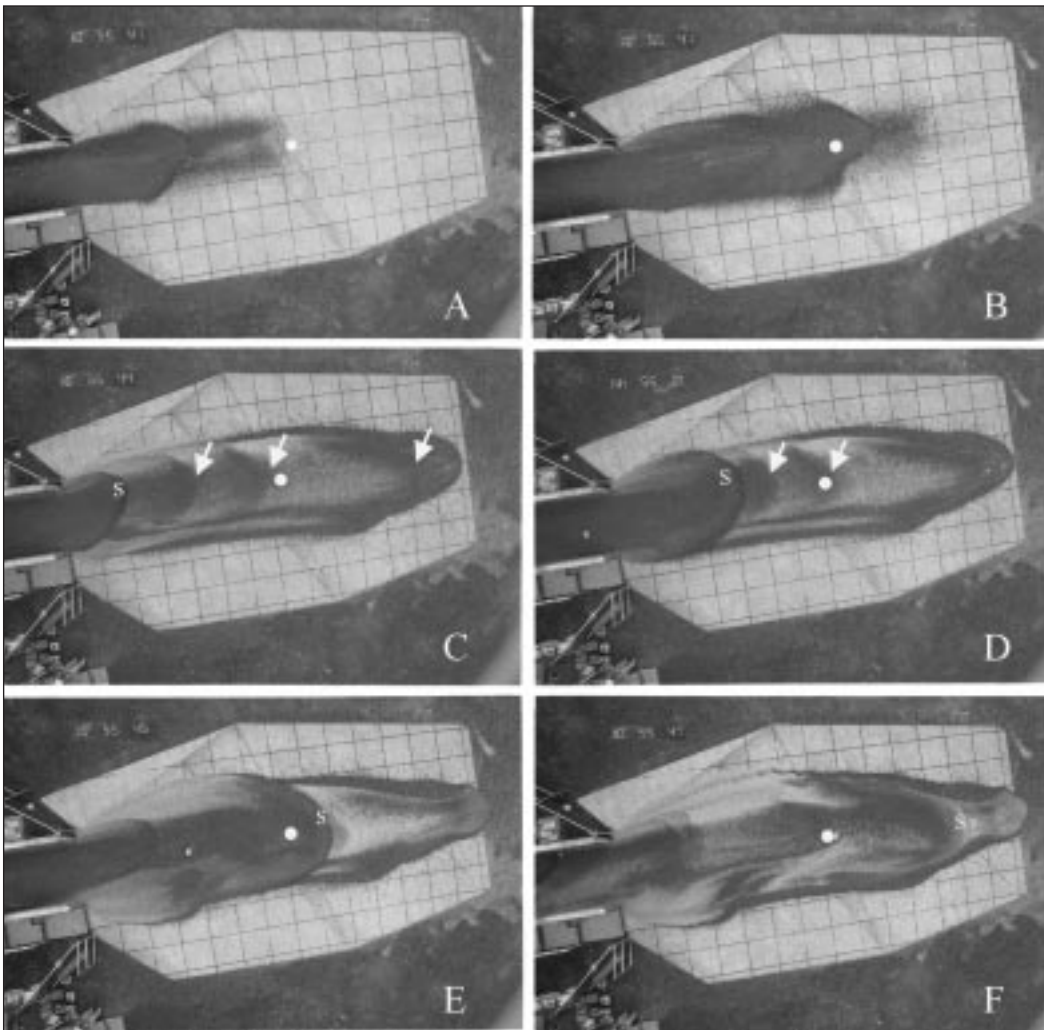


**Figure 3.** Sequence of aerial photographs illustrating deposition of an experimental debris flow on the runout surface. The time between successive frames ranges from about 1 to 3 s; the total elapsed time is about 6 s. A 1 m grid provides scale. Note that surges deposit sediment progressively in this experiment. One large surge (s) sweeps across the deposit, and clusters of surface gravel (arrows) mark the fronts of prior surges. An instrumentation port (white dot) is located along the centerline of the runout area 7.5 m beyond the flume mouth. See Major (1997) for a more detailed photographic sequence.

places overlain by less well-sorted sandy debris (cf. Major, 1997, Fig. 8D), and surfaces of deposits had clusters of gravel that represented arrested fronts of surge waves (Fig. 3). Lateral and distal margins of deposits contained more abundant surface gravel than did adjacent debris within a few tens of centimeters (cf. Major, 1997, Figs. 6 and 9), but the margins did not consist solely of well-sorted gravel. Despite apparent particle segregation during flow, the sedimentary characteristics of the debris adjacent to margins of deposits were not substantially different from those farther away from margins. Indeed, grain-size analyses revealed no significant variation in the sediments that composed the lateral and distal edges of deposits and only minor variations between deposit edges and adjacent interior sediments (Major, 1996). Therefore, the sedimentologic characteristics of lateral margins of deposits were similar to those at the distal toe, and only the outermost edge of a deposit and the buried leading edge of a flow contained a distinct concentration of the coarsest clasts.

#### **BASAL FLUID PRESSURE AND TOTAL BED-NORMAL STRESS**

Fluid pressure and total bed-normal stress were measured simultaneously at the base of several experimental debris flows and deposits to characterize conditions during debris-flow motion, deceleration, and deposition. Sensors were located along the centerline of the flume channel 67 m below the re-

lease gate (Fig. 1), along the centerline of the runout area 7.5 m beyond the flume mouth (Fig. 3), and, in one experiment, 14.5 m beyond the flume mouth. The proximity of fluid-pressure and total-stress sensors is illustrated in Figure 4. We measured bed-normal stress with an S-beam load cell rigidly affixed to a circular 500 cm<sup>2</sup> sensor plate mounted flush with the bed (cf. Iverson et al., 1992; Iverson, 1997a) (Fig. 4). Measurements of fluid pressure employed screened, rapid response, differential-pressure transducers (vented to the atmosphere) similar to those used by Iverson and LaHusen (1989). The port connecting pressure transducers to sensor plates was filled with water and covered with a saturated, highly conductive, sintered-stone filter or 230-mesh screen to provide rapid, direct hydraulic connection to pore fluid at the base of the experimental debris (Fig. 4A). An infrared laser suspended over the sensor plate in the flume channel precisely measured temporal variations of the depth of the moving flow (Iverson, 1997a). Comparable measurements of flow-depth variation in the depositional area beyond the flume exist for a limited number of experiments. Sensor signals were logged by computers at rates that varied from 1000–2000 Hz along the flume channel to 1–1000 Hz in the runout area beyond the flume. Experiments were filmed and photographed from several angles, and several videotape images were imprinted with digital times by using a high-precision timer synchronized with the data-acquisition systems. These images allowed us to correlate flow appearance with the recorded fluid-pressure and bed-stress data.

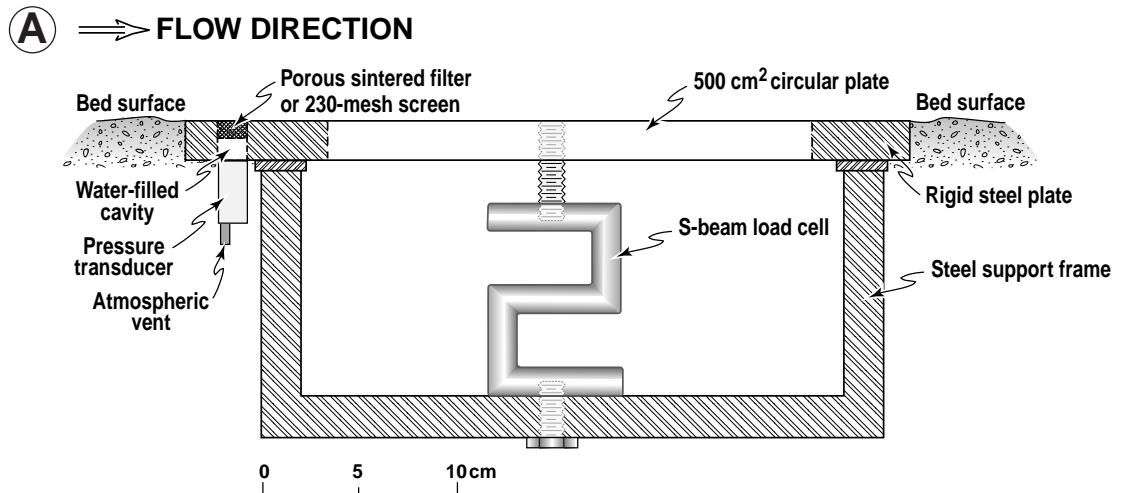


**Figure 4.** Instrument configuration for measuring pore-fluid pressure and bed-normal stress simultaneously. (A) Schematic cross section of instrumentation. A 500 cm<sup>2</sup> circular plate is rigidly affixed to an S-beam load cell mounted beneath the plate and is free to deflect normal to the bed. A fluid-pressure transducer is attached to the rigid steel plate adjacent to the load-cell plate. (B) Instrumentation plate excavated from beneath a deposit that blankets the runout surface at the debris-flow flume. Deposit over the plate was 12.5 cm thick. An arrow marks the position of the fluid-pressure sensor.

**Flume Channel**

Iverson (1997a, 1997b) presented time series of basal pore pressures and total bed-normal stresses in rapidly moving experimental debris flows that completely swept past measurement cross sections. Temporal variations in the data reflect spatial changes that occur from the head to the tail of a de-

bris flow. For flows having an average speed of 10 m/s, signal variations within 0.1 s represent spatial variations along a 1 m segment of the flow.

As shown by Iverson (1997a, 1997b), fluid pressure and total normal stress at the channel bed correspond with, and respond rapidly to, fluctuations in flow depth that result from passage of surge waves (Fig. 5). Total bed-normal stress increases proportionately with flow depth, except during

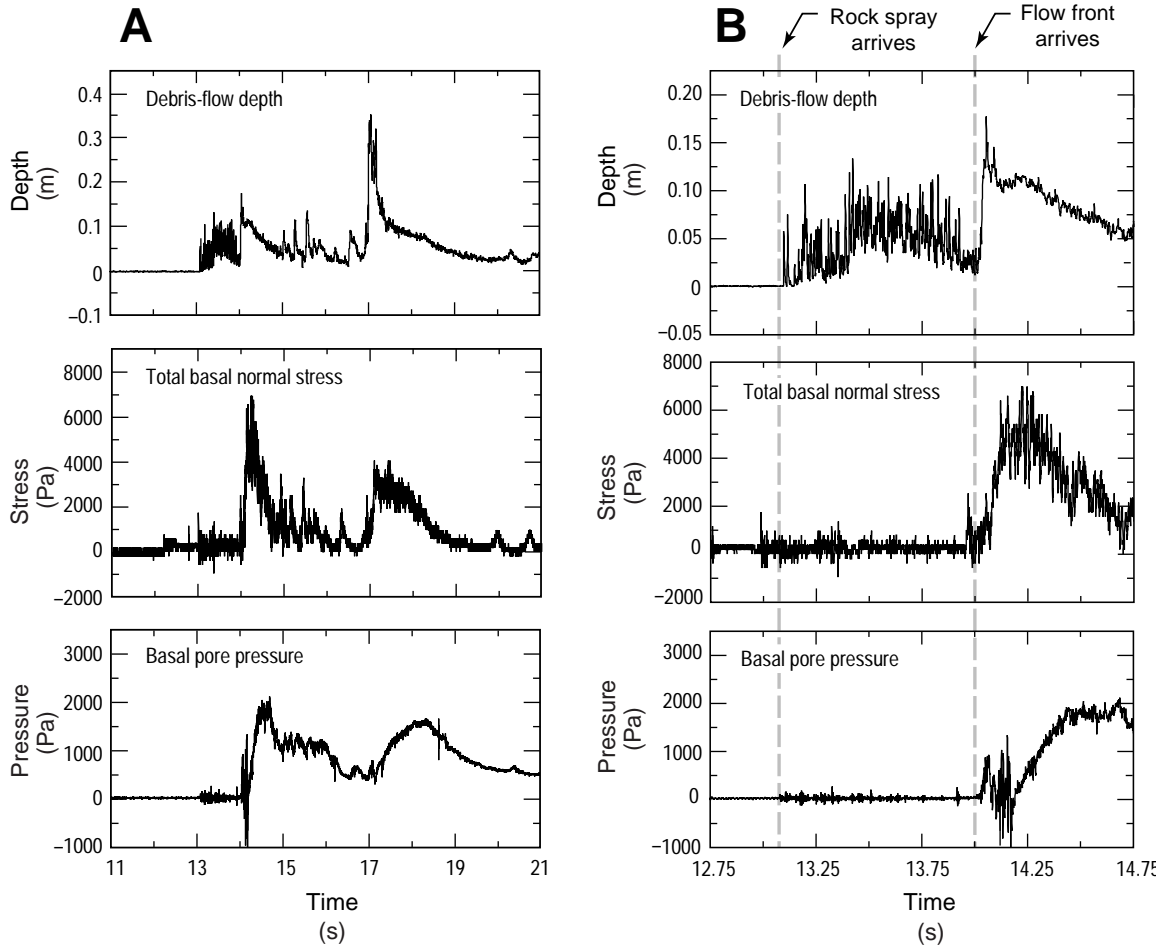


**Figure 5.** Representative measurements of flow depth, total basal normal stress, and basal fluid pressure made at the channel bed 67 m downslope from the release gate (from Iverson, 1997b). Data are for a debris flow of 9 m<sup>3</sup> of water-saturated loamy gravel released in experiment 083194. (A) Data for the entire event duration. (B) Expanded time base showing details during arrival of the debris flow front. Pore pressure does not rise appreciably until the deepest part of the flow front passes the sensor plate.

brief intervals when significant momentum flux normal to the bed occurs. Basal fluid pressure, on the other hand, is close to zero near the flow front and increases only after the flow front has passed (Fig. 5B). Basal fluid pressure behind the flow front approaches and sometimes slightly exceeds levels sufficient to liquefy the sediment. These data confirm a common impression gained from observations of many natural debris flows: surge heads typically are relatively dry, whereas debris masses behind surge heads are saturated with water and appear liquefied (e.g., Singewald, 1928; Sharp and Nobles, 1953; Okuda et al., 1981; Costa and Williams, 1984; Pierson, 1986).

### Runout Area

Beyond the flume mouth, measured basal fluid pressure and total bed-normal stress reflect conditions that evolve during flow deceleration and deposition. Temporal variation of these data, however, does not correspond to simple spatial variation from the debris-flow head to tail, as it does within the flume channel. Initially, the data characterize basal fluid pressure and bed-normal stress near the front of a decelerating debris flow. Within seconds, however, debris begins to accumulate (cf. Major, 1997; Fig. 3); thereafter, data represent pore pressure and stress developed in a rapidly thickening pile of deposited sediment. Progressively increasing fluid pressure and

bed-normal stress during deposition (Fig. 6) corroborate observations that the experimental deposits formed primarily by incremental accretion of sediment (Major, 1997). Following deposition, the data document basal fluid pressure and total bed-normal stress in a quasi-statically consolidating debris slurry (Fig. 6, A, B, D, and E). Owing to variations in deposit geometry and runout distance (Major, 1997), the location of the sensor plate relative to the distal extent of the flow front varied among experiments. In one experiment (090198), the flow front came to rest directly over the sensor plate located 7.5 m beyond the flume mouth (Fig. 7). In another experiment (091395), the flow traveled far enough across the runout area that we measured basal fluid pressure and total bed-normal stress during passage of the flow front at two locations (7.5 m and 14.5 m) beyond the flume (Fig. 6, F and G). Despite variable runout distances among experiments, our measurements revealed the salient characteristics of the basal pore-fluid pressures and bed-normal stresses that existed in the debris flows during deceleration and deposition.

Overall, our data demonstrate that flow fronts in the runout area, as in the flume channel (Iverson, 1997a), commonly lacked high pore-fluid pressure. This finding was most clearly demonstrated in experiment 090198 (Fig. 6H), in which the flow front stopped directly over the sensor port (Fig. 7). In that experiment, total bed-normal stress rose abruptly upon arrival of the flow

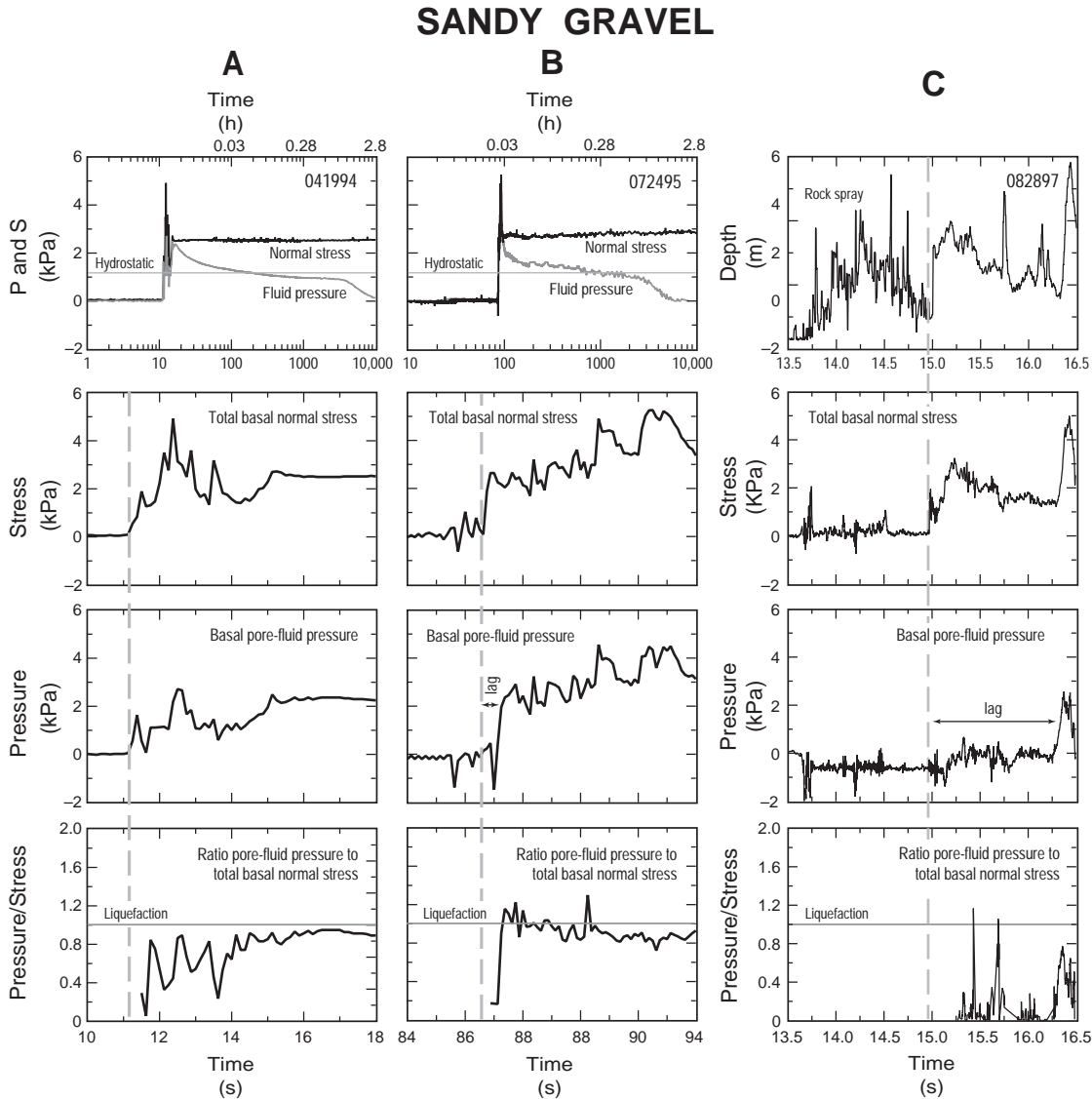


**Figure 6. Representative measurements of total basal normal stress and basal fluid pressure made in the runout area beyond the flume mouth. Plots illustrate details during arrival of the flow front and, for some experiments, show measurements through postdepositional consolidation. Although flow depth is not available for all experiments (see Appendix 1), a vertical dashed line indicates arrival of the flow front. All data are for debris flows having volumes that ranged from 8.5 to 10 m<sup>3</sup>. For A–C, the experimental debris consisted of sandy gravel containing about 1% mud (silt + clay). For D–H, the experimental debris consisted of loamy gravel containing about 2% to 10% mud. The debris for experiment 082897 (C) contained 6 vol% large clasts averaging 150 mm diameter.**

front, but fluid pressure rose negligibly, showing that the flow front was largely unsaturated. Our data also show that within about 1 m of most flow fronts, basal fluid pressure rose rapidly and in some flows was sufficient to liquefy the debris (Fig. 6, B, D, and E). Behind the flow fronts, crests and troughs in fluid pressure were essentially in phase with, and of comparable magnitude to, the measured total bed-normal stress (Fig. 6).

Basal bed-normal stress and fluid pressure measured behind flow fronts during flow deceleration generally increased proportionately; however, variation occurred among flows (Fig. 6). One flow of sandy gravel (041994, Fig. 6A) exhibited nearly simultaneous increases in fluid pressure and bed-normal stress despite a pronounced lag between signals at the channel bed a mere 25 m upslope (R. M. Iverson, unpub. data). Another flow of similar

composition (072495, Fig. 6B) exhibited a pronounced lag between signals: arrival of the flow front was marked by an abrupt rise of bed-normal stress (for justification of using bed-normal stress to infer flow-front arrival, see Appendix 1) whereas an analogous abrupt rise of fluid pressure was delayed by about 0.5 s. A similar lag between the rise in bed-normal stress and fluid pressure was observed in a third sandy-gravel flow that contained 150-mm-diameter clasts (082897, Fig. 6C). In that experiment, however, fluid pressure rose abruptly only after a large saturated wave arrived and overran the decelerating flow front.

Relationships between bed-normal stress and fluid pressure in the finer-grained loamy-gravel flows were similar to those measured in coarser-grained flows. In two experiments (052694 and 083194, Fig. 6, D and E),

## LOAMY GRAVEL

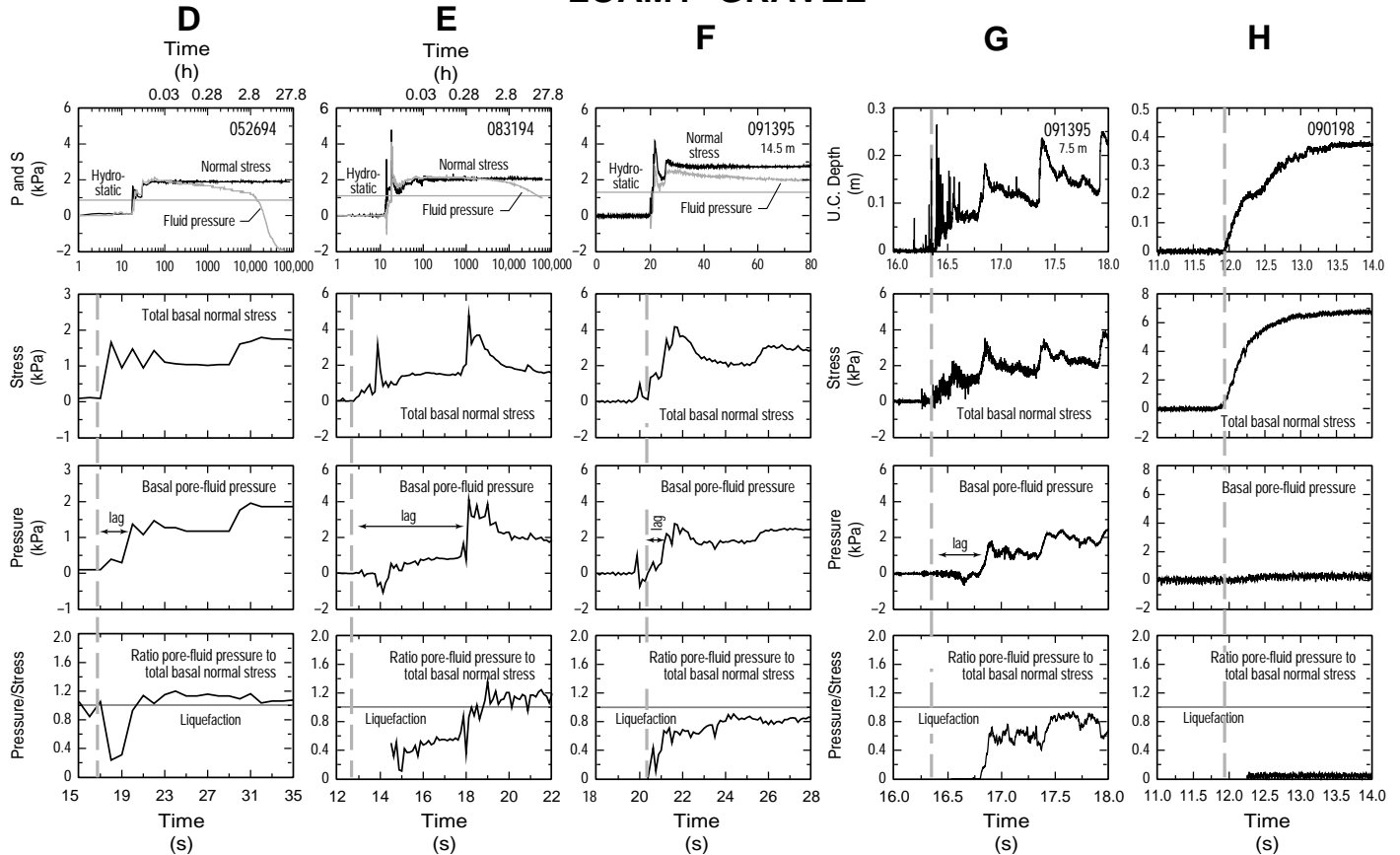


Figure 6. (Continued).

abrupt rises in fluid pressure lagged behind the abrupt changes of bed-normal stress that marked flow-front arrivals by as much as 2–5 s. In subsequent experiments with similar debris (e.g., 091395, Fig. 6, F and G), lags between abrupt rises in bed-normal stress and basal fluid pressure were evident but less pronounced (~0.5 s).

Temporal relationships between measured basal fluid pressure and bed-normal stress show greater variation in the runout area than along the channel bed in the lower flume. This variability may be related in part to differences in sampling rates at the two locations. In the flume channel, sampling rates ranged from 1000–2000 Hz; lags between changes in bed-normal stress and fluid pressure commonly were  $\leq 1$  s, but were easily detected (Iverson, 1997a). In contrast, some flows were sampled at frequencies as low as 1 Hz in the runout area. Measured lags between bed-normal stress and fluid pressure in the runout area are real; however, some experiments for which there is no measured lag (Fig. 6A) may actually have a lag of  $< 1$  s that was undetected.

## DISCUSSION

A new mechanical model—which treats debris flows as variably liquefied Coulomb mixtures in which pore-fluid pressure mediates flow resistance owing to intergranular friction (Iverson, 1997a, 1997b)—provides a framework in which to interpret our measurements of fluid pressure and bed-normal stress during flow deceleration and deposition. In the absence of fluid pressure, the model describes forces in a deforming Coulomb ma-

terial. If the mass is completely liquefied by fluid pressure, the model describes forces in a viscous fluid flow. With a variable pore-pressure field, the model describes forces in a deforming granular mass that can exhibit both solid and fluid behavior. Resistance is focused in unliquefied regions of compressing flow where the material acts like a Coulomb solid and supports high lateral stresses; liquefied regions where the debris acts like a fluid or less resistance.

Our data support the model of Iverson (1997a, 1997b) and reinforce two of his findings regarding the distribution of pore-fluid pressure in debris flows: (1) fluid pressure rises abruptly *after* passage of the flow front and (2) fluid pressure approaches levels sufficient to liquefy the debris. Moreover, our data show that high interior pore-fluid pressures can persist through deposition, but can vary significantly among events. At measurement locations beyond the flume, basal fluid pressure in many flows balanced a significant fraction of the total bed-normal stress behind flow fronts; in other flows, fluid pressure rose barely above hydrostatic level before sediment accumulated (e.g., Fig. 6C). In two loamy-gravel debris flows (Fig. 6, D and E), fluid pressure appeared to slightly exceed levels sufficient to liquefy the debris during deceleration and deposition. Consolidation theories that couple fluid pressure and stress fields provide a possible explanation for these particularly high fluid pressures. Such theories have shown that fluid pressure may initially rise to levels greater than anticipated from the degree of loading (e.g., Gibson et al., 1963; Schiffman et al., 1969). This phenomenon, known as the Mandel-Cryer effect, results from multidimensional strain in a consolidating body even while pore-fluid flow is one-dimen-

sional. Because stress and strain fields must remain compatible throughout the debris flow, lateral strains developed in locally drained soil elements transfer stresses to adjacent, undrained soil elements. Such stress transfers effectively “squeeze” adjacent soil elements and cause fluid pressure to rise temporarily to a level greater than anticipated from the degree of loading. Minor drift of either the load cell or the pressure-transducer calibration can also cause the fluid-pressure-to-bed-stress ratio to appear to exceed the liquefaction threshold. Nevertheless, fluid pressure behind flow fronts in the runout area typically balanced about 80% or more of the total bed-normal stress. Therefore, most of our experimental debris flows deposited sediment even while flow interiors remained nearly liquefied.

Sediment deposition that occurs while flow interiors remain nearly liquefied is incompatible with the hypothesis that spatially uniform dissipation of excess fluid pressure causes debris-flow deposition (Terzaghi, 1956; Hutchinson, 1986). Furthermore, the nearly liquefied state of most of the deposited debris shows that deposits initially have little strength except along their margins. In such cases, intrinsic viscoplastic yield strength cannot be invoked to explain debris-flow deposition. One ramification of this finding is that deposit thickness cannot be used to reconstruct the yield strength of a debris flow, contrary to a common practice that is based on the precept that debris flows behave as Bingham viscoplastic materials (e.g., Johnson, 1970, 1984; Fink et al., 1981; Major and Voight, 1986; Rodolfo et al., 1989; Whipple and Dunne, 1992; Kim et al., 1995; Coussot and Proust, 1996).

Although the experimental debris flows discussed in this work lasted only a few tens of seconds, the high fluid pressure that is characteristic of debris-flow interiors is unlikely to dissipate substantially even over the duration of typical natural debris flows. The characteristic time needed to dissipate excess pore-fluid pressure in a debris flow is given by  $h^2/D$ , where  $h$  is the flow depth and  $D$  is the hydraulic diffusivity of the debris, which depends on mixture permeability and compressibility and on pore-fluid viscosity (cf. Major et al., 1997; Iverson, 1997a, 1997b; Major, in press). Diffusivities of debris-flow slurries having widely ranging compositions have been estimated from gravity-driven consolidation tests and from analysis of long-term changes of fluid pressure in the experimental debris-flow deposits (cf. Fig. 6, A, B, D, and E; Major et al., 1997; Major, in press). Values of  $D$  ranged from about  $10^{-4}$  m<sup>2</sup>/s for the sandy-gravel deposits to  $10^{-7}$  m<sup>2</sup>/s for mixtures containing greater amounts of fine debris. For debris-flow depths of 0.5 to 10 m and for  $D$  values on the order of  $10^{-6}$  m<sup>2</sup>/s, diffusion of excess fluid pressure requires tens of hours to hundreds of days, times that far exceed durations of most debris flows. These pressure-dissipation times are inferred from the behavior of quasi-statically consolidating slurries rather than from rapidly flowing debris, but they place an upper bound on times that may be characteristic of debris flows. For rapidly flowing debris, hydraulic diffusivities are probably larger, but even if they are as much as two to three orders of magnitude larger, characteristic pressure-dissipation times remain on the order of tens of minutes to tens of hours (Iverson, 1997a). Hence, most natural debris flows are likely to deposit sediment that is mostly liquefied but impounded by high-friction debris at flow margins.

Our observation that the finer-grained experimental flows produced the thinnest deposits (cf. Major, 1997) further illustrates that localized flow resistance, affected by Coulomb friction and pore-fluid pressure, dominates debris-flow deposition. This observation seems counterintuitive in light of rheometric experiments that show that apparent yield strength of slurries increases (at a given sediment concentration) as their fines content increases (e.g., Major and Pierson, 1992). On the basis of rheometric results, one expects that finer-grained debris flows should produce thicker deposits compared to coarser-grained flows; however, the opposite is commonly observed (e.g., Fryxell and Horberg, 1943; Whipple and Dunne, 1992; Johnson, 1997). Apparently, the lower permeability and greater compressibility (i.e., lower diffusivity) of the finer-grained debris helps sustain high pore-fluid pressure,



**Figure 7. Snout of experimental deposit 090198, which came to rest on top of the instrumentation port located 7.5 m beyond the flume mouth and almost directly beneath the top of the meter stick shown in the photograph. Fluid pressure rose negligibly upon deposition, showing that the flow front was largely unsaturated (cf. Fig. 6H).**

even near margins, for a longer period (cf. Fig. 6, A and B, with Fig. 6, D and E); sustained high pore pressure reduces frictional resistance and allows finer-grained debris to spread more thinly. Of course, debris flows that contain abundant fine sediment in the matrix can form thick deposits if coarse clasts are concentrated at the margins (e.g., Johnson, 1997).

A variety of additional evidence supports the idea that debris-flow deposition is controlled by frictional resistance focused at flow fronts. Okuda et al. (1981) placed groundwater sensors along the paths of debris flows on an alluvial fan and found that water did not infiltrate vertically into the channel bed during flow passage. Therefore, frictional resistance was not enhanced by basal fluid escape from moving flows. Furthermore, they found that debris-flow fronts were relatively dry. They inferred that lateral escape of fluid at the flow front increased friction and stimulated flow deceleration and deposition. Our experiments reveal that fluid does not need to escape the flow front; instead, the flow front is composed of debris that lacks much interstitial fluid throughout most of the flow duration. Pierson (1984) observed that the coarsest clasts commonly moved to the front and lateral margins of debris flows and that deposits commonly contained rims of coarse, clast-supported gravel that surrounded finer-grained debris. He noted that such marginal rims commonly have an openwork structure and are well drained and dominated by frictional contact. He further observed that when the clastic rim was removed from fresh deposits and the sediment behind the rim agitated, liquefied debris would flow out and eventually form a thinner deposit (T. C. Pierson, 1997, personal commun.). Curry (1966) observed similar behavior of freshly deposited debris. On the basis of such observations, Pierson (1984) proposed that when driving stresses could no longer overcome the strength of the marginal rim, the debris flow stopped, effectively dammed behind a retaining wall. Conversely, Mohrig et al. (1998) observed that the fronts of subaqueous experimental debris flows, composed of nearly equal mixtures of sand and silt, accelerated rapidly and sometimes detached from flow bodies if the flow fronts hydroplaned over the substrate. Hydroplaning occurred as a result of high basal fluid pressure developed at the flow front. Thus, when high fluid pressure is developed at the flow front, flow resistance markedly declines.

Measurements of fluid pressure following deposition of the experimental flows confirm that excess fluid pressure dissipates significantly only during postdepositional consolidation (Fig. 6, A, B, D, and E; Major, in press). Variations in pressure-dissipation times among deposits were caused primarily by variations of debris composition; deposit thicknesses among experiments were similar (cf. Major, 1997). Small amounts of mud significantly alter debris permeability, impeding dissipation of excess fluid pressure (Major et al., 1997; Major, in press). In the sandy-gravel deposits, postdepositional drainage occurred rapidly, and excess fluid pressure dissipated within tens of seconds to several minutes after sediment deposition (e.g., Fig. 6, A and B). In contrast, fluid pressure in the loamy-gravel deposits remained nearly lithostatic for several minutes to several tens of minutes and exceeded hydrostatic pressure for several hours (e.g., Fig. 6, D and E).

Major (1996) calculated the distribution of fluid pressure and frictional stress developed near the margins of thin, wide, two-dimensional homogeneous deposits. He found that consolidation of such deposits was a mostly one-dimensional, vertical process when the width-to-thickness ratio of the deposit was greater than 5. In fully saturated domains having physical properties commensurate with those of many debris-flow deposits (e.g., Major et al., 1997), excess fluid pressure dissipated quickly—and frictional stress increased—only along marginal zones that were half as wide as the domain was thick. Numerical results revealed that excess fluid pressure can remain elevated—and frictional stress depressed—everywhere except at deposit margins for time scales that range from several minutes to perhaps several days in debris-flow deposits that are 1 m thick. The significance of Major's (1996) numerical results is that even if excess fluid pressure existed uniformly throughout a homogeneous debris flow during transport, it would be unlikely to decay anywhere except along the flow margin over time scales relevant to debris-flow events.

## CONCLUSIONS

Measurements of pore-fluid pressure and total bed-normal stress at the base of 10 m<sup>3</sup> experimental debris flows show that pore-pressure magnitudes nearly sufficient to cause liquefaction persist in flow interiors during deceleration and sediment deposition. Excess pore-fluid pressure in debris-flow interiors dissipates significantly only during postdepositional consolidation. In contrast, leading edges of flows exhibit negligible positive pore-fluid pressure. Therefore, debris-flow deposition results from grain-contact friction and bed friction concentrated along the flow perimeter, where high pore-fluid pressure is absent. Focused frictional resistance can occur in relatively homogeneous debris flows, but is enhanced if margins are composed predominantly of coarse clasts. This finding contradicts models that invoke widespread decay of excess pore-fluid pressure, intrinsic viscoplastic yield strength, or pervasive grain-collision stresses to explain debris-flow deposition. Because deposition results from frictional resistance focused at flow margins, deposit thickness cannot be used to infer an intrinsic yield strength of moving debris.

## ACKNOWLEDGMENTS

The experiments reported herein were labor intensive and could not have been completed without the help of Rick LaHusen, Tony Bequette, Kevin Hadley, Matthew Logan, Kelly Swinford, and Winston Stokes. We deeply appreciate their commitment to the success of this work. We are also grateful for additional assistance during various experiments provided by Jim Vallance, Carl Zimmerman, Brooke Fiedorowicz, Mark Reid, Colleen Riley, Gordon Stratford, Tom Lill, and Ben Schonfeld. Discussions with Tom Dunne, David McTigue, Jim Vallance, and Rick LaHusen contributed to clarification of ideas presented in this work. David Mohrig, Sue Cannon,

Jim O'Connor, Y. K. Sohn, Harvey Kelsey, and Bob Webb provided thoughtful criticisms of an earlier draft of this paper.

## APPENDIX 1.

In some experiments, we lack measurements of flow depth in the runout area. In such experiments, we infer flow-front arrival from abrupt changes in total bed-normal stress and from analysis of videotape recordings. Owing to the lack of flow-depth data, we must assess the quality of the stress measurements in order to compare them with fluid pressure during flow deceleration and deposition. We evaluate whether the measured total bed-normal stresses are reasonable by calculating deposit bulk densities. Total bed-normal stress ( $\sigma_{\text{total}}$ ) is related to total bulk density ( $\rho_t$ ), gravitational acceleration ( $g$ ), and deposit thickness ( $h$ ) by  $\sigma_{\text{total}} = \rho_t g h$ . Our estimates of the deposit's average bulk densities from measured total bed-normal stresses and deposit thicknesses (cf. Major, 1997) are comparable to bulk densities measured directly by sampling (cf. Iverson, 1997a). For example, the average total basal bed-normal stress of deposit 041994 (Fig. 6A) was 2.5 kPa. The deposit was 0.12 m thick. Therefore, the estimated average total bulk density of the deposit was 2100 kg/m<sup>3</sup>. By definition, the total bulk density of a saturated granular mass is given by  $\rho_t = \rho_f \phi + \rho_s (1 - \phi)$ , where  $\rho_f$  and  $\rho_s$  are the densities of the pore fluid and solid particles, respectively, and  $\phi$  is deposit porosity. Using the calculated value of total bulk density and solving this expression for porosity yields  $\phi = 0.32$ , a reasonable estimate for the porosity of sandy debris. The dry bulk density of the deposit, given by  $\rho_s (1 - \phi)$ , is 1800 kg/m<sup>3</sup> if we assume that  $\rho_s = 2650$  kg/m<sup>3</sup>. The estimated dry bulk density obtained from hand sampling of the deposit ranged from 1870 to 1930 kg/m<sup>3</sup> (Iverson, 1997a), in good agreement with that estimated from measured total bed-normal stress.

Total bed-normal stresses measured along the flume channel varied directly with flow depth, and the inferred average bulk density of flowing debris was comparable to deposit bulk density (Iverson, 1997a). Thus, we infer that bulk densities of decelerating flows were comparable to those of deposits and that fluctuations in total bed-normal stress in the runout area corresponded directly with changes in flow depth. We therefore infer the arrival of flow fronts and subsequent surge waves from the measured bed-normal stresses. Our inferences are supported by the synchronized videotape record and by the experiments in which we measured flow depth in the runout area (Fig. 6, C, G, and H).

## REFERENCES CITED

- Bagnold, R. A., 1954, Experiments on a gravity-free dispersion of large solid spheres in a Newtonian fluid under shear: Royal Society of London Proceedings, ser. A, v. 225, p. 49–63.
- Beatty, C. B., 1974, Debris flows, alluvial fans, and a revitalized catastrophism: *Zeitschrift für Geomorphologie*, supplement, v. 21, p. 39–51.
- Blackwelder, E., 1928, Mudflow as a geologic agent in semiarid mountains: *Geological Society of America Bulletin*, v. 39, p. 465–480.
- Blair, T. C., and McPherson, J. G., 1994, Alluvial fan processes and forms, in Abrahams, A. D., and Parsons, A. J., eds., *Geomorphology of desert environments*: London, Chapman and Hall, p. 354–402.
- Broscoe, A. J., and Thomson, S., 1969, Observations on an alpine mudflow, Steele Creek, Yukon: *Canadian Journal of Earth Sciences*, v. 6, p. 219–229.
- Casagrande, A., 1936, Characteristics of cohesionless soils affecting the stability of slopes and earth fills: *Boston Society of Civil Engineers Journal*, v. 23, p. 13–32.
- Costa, J. E., and Jarrett, R. D., 1981, Debris flows in small mountain stream channels of Colorado and their hydrologic implications: *Bulletin of the Association of Engineering Geologists*, v. 18, p. 309–322.
- Costa, J. E., and Williams, G. P., 1984, Debris-flow dynamics (video tape): U.S. Geological Survey Open-File Report 84-606, 22 min.
- Coussot, P., and Proust, S., 1996, Slow unconfined spreading of a mudflow: *Journal of Geophysical Research*, v. 101, p. 25217–25229.
- Curry, R. R., 1966, Observation of alpine mudflows in the Tenmile Range, central Colorado: *Geological Society of America Bulletin*, v. 77, p. 771–776.
- DeGraff, J., 1994, The geomorphology of some debris flows in the southern Sierra Nevada, California: *Geomorphology*, v. 10, p. 231–252.
- Eckersley, J. D., 1990, Instrumented laboratory flowslides: *Geotechnique*, v. 40, p. 489–502.
- Fink, J. H., Malin, M. C., D'Alli, R. E., and Greeley, R., 1981, Rheological properties of mudflows associated with the spring 1980 eruptions of Mount St. Helens volcano, Washington: *Geophysical Research Letters*, v. 8, p. 43–46.
- Folk, R. L., 1984, *Petrology of sedimentary rocks*: Austin, Texas, Hemphill, 184 p.
- Fryxell, F. M., and Horberg, L., 1943, Alpine mudflows in Grand Teton National Park, Wyoming: *Geological Society of America Bulletin*, v. 54, p. 457–472.
- Gibson, R. E., Knight, K., and Taylor, P. W., 1963, A critical experiment to examine theories of three-dimensional consolidation, in *Problems of settlements and compressibility of soils*, Proceedings of the European Conference on Soil Mechanics and Foundation Engineering: Wiesbaden, Germany, v. 1, p. 69–76.
- Gori, P. L., and Burton, W. C., 1996, Debris-flow hazards in the Blue Ridge of Virginia: U.S. Geological Survey Fact Sheet 159-96, 4 p.

- Hampton, M. A., 1979, Buoyancy in debris flows: *Journal of Sedimentary Petrology*, v. 49, p. 753–758.
- Harris, S. A., and Gustafson, C. A., 1993, Debris flow characteristics in an area of continuous permafrost, St. Elias Range, Yukon Territory: *Zeitschrift für Geomorphologie*, v. 37, p. 41–56.
- Hubert, J. F., and Filipov, A. J., 1989, Debris-flow deposits in alluvial fans on the west flank of the White Mountains, Owens Valley, California, USA: *Sedimentary Geology*, v. 61, p. 177–205.
- Hutchinson, J. N., 1986, A sliding-consolidation model for flow slides: *Canadian Geotechnical Journal*, v. 23, p. 115–126.
- Inman, D. L., 1952, Measures for describing the size distribution of sediments: *Journal of Sedimentary Petrology*, v. 22, p. 125–145.
- Iverson, R. M., 1997a, The physics of debris flows: *Reviews of Geophysics*, v. 35, p. 245–296.
- Iverson, R. M., 1997b, Hydraulic modeling of unsteady debris-flow surges with solid-fluid interactions, in Chen, C. L., ed., *Debris flow hazards mitigation: Mechanics, prediction, and assessment: American Society of Civil Engineers, Proceedings of First International Conference, August 7–9, San Francisco*, p. 550–560.
- Iverson, R. M., and LaHusen, R. G., 1989, Dynamic pore-pressure fluctuations in rapidly shearing granular materials: *Science*, v. 246, p. 796–799.
- Iverson, R. M., and LaHusen, R. G., 1993a, Friction in debris flows: Inferences from large-scale flume experiments, in Shen, H. W., Su, S. T., and Wen, F., eds., *Hydraulic Engineering '93, Proceedings of ASCE 1993 conference, San Francisco, California, July 25–30*, p. 1604–1609.
- Iverson, R. M., and LaHusen, R. G., 1993b, Pore-pressure dynamics in debris-flow experiments [abs.]: *Eos (Transactions, American Geophysical Union)*, v. 74, p. 310.
- Iverson, R. M., LaHusen, R. G., and Costa, J. E., 1992, Debris-flow flume at H. J. Andrews Experimental Forest, Oregon: U.S. Geological Survey Open-File Report 92-483, 2 p.
- Iverson, R. M., LaHusen, R. G., Major, J. J., and Zimmerman, C. L., 1994, Debris flow against obstacles and bends: Dynamics and deposits [abs.]: *Eos (Transactions, American Geophysical Union)*, v. 75, p. 274.
- Iverson, R. M., Reid, M. A., and LaHusen, R. G., 1997, Debris-flow mobilization from landslides: *Annual Review of Earth and Planetary Sciences*, v. 25, p. 85–138.
- Jahns, R. H., 1949, Desert floors: *California Institute of Technology, Engineering and Science Newsletter*, v. 12, p. 10–14.
- Johnson, A. M., 1970, *Physical processes in geology*: San Francisco, Freeman, Cooper, and Co., 576 p.
- Johnson, A. M., 1984, Debris flow, in Brunsden, D., and Prior, D. B., eds., *Slope instability: New York, John Wiley and Sons*, p. 257–361.
- Johnson, S. E., 1997, The 1996 Tumalt Creek debris flows and debris avalanches in the Columbia River Gorge east of Portland, Oregon, in Chen, C. L., ed., *Debris flow hazards mitigation: Mechanics, prediction, and assessment: American Society of Civil Engineers, Proceedings of First International Conference, August 7–9, San Francisco*, p. 395–404.
- Kim, S. B., Chough, S. K., and Chun, S. S., 1995, Bouldery deposits in the lowermost part of the Cretaceous Kyokpori Formation, SW Korea: Cohesionless debris flows and debris falls on a steep-gradient delta slope: *Sedimentary Geology*, v. 98, p. 97–119.
- Laberg, J. S., and Vorren, T. O., 1995, Late Weichselian submarine debris flow deposits on the Bear Island Trough Mouth Fan: *Marine Geology*, v. 127, p. 45–72.
- Lowe, D. R., 1976, Grain flow and grain flow deposits: *Journal of Sedimentary Petrology*, v. 46, p. 188–199.
- Major, J. J., 1996, Experimental studies of deposition by debris flows: Process, characteristics of deposits, and effects of pore-fluid pressure [Ph.D. thesis]: Seattle, University of Washington, 341 p.
- Major, J. J., 1997, Depositional processes in large-scale debris-flow experiments: *Journal of Geology*, v. 105, p. 345–366.
- Major, J. J., 1998, Pebble orientation on large experimental debris-flow deposits: *Sedimentary Geology*, v. 117, p. 151–164.
- Major, J. J., in press, Gravity-driven consolidation of granular slurries: Implications for debris-flow deposition and deposit characteristics: *Journal of Sedimentary Research*.
- Major, J. J., and Pierson, T. C., 1992, Debris flow rheology: Experimental analysis of fine-grained slurries: *Water Resources Research*, v. 28, p. 841–857.
- Major, J. J., and Voight, B., 1986, Sedimentology and clast orientations of the 18 May 1980 southwest flank lahars, Mount St. Helens, Washington: *Journal of Sedimentary Petrology*, v. 56, p. 691–705.
- Major, J. J., Iverson, R. M., McTigue, D. F., Macias, S., and Fiedorowicz, B. K., 1997, Geotechnical properties of debris-flow sediments and slurries, in Chen, C. L., ed., *Debris flow hazards mitigation: Mechanics, prediction, and assessment: American Society of Civil Engineers, Proceedings of First International Conference, August 7–9, San Francisco*, p. 249–259.
- Masson, D. G., Huggert, Q. J., and Brunsden, D., 1993, The surface texture of the Saharan debris flow deposit and some speculations on submarine debris flow processes: *Sedimentology*, v. 40, p. 583–598.
- Middleton, G. V., and Hampton, M. A., 1976, Subaqueous sediment transport and deposition by sediment gravity flows, in Stanley, D. J., and Swift, D. J. P., eds., *Marine sediment transport and environmental management*: New York, John Wiley and Sons, p. 197–218.
- Mohrig, D., Whipple, K. X., Hondzo, M., Ellis, C., and Parker, G., 1998, Hydroplaning of subaqueous debris flows: *Geological Society of America Bulletin*, v. 110, p. 387–394.
- Morton, D. M., and Campbell, R. H., 1974, Spring mudflows at Wrightwood, southern California: *Quarterly Journal of Engineering Geology*, v. 7, p. 377–384.
- Nemec, W., and Steel, R. J., 1984, Alluvial and coastal conglomerates: Their significant features and some comments on gravelly mass-flow deposits, in Koster, E. H., and Steel, R. J., eds., *Sedimentology of gravels and conglomerates: Canadian Society of Petroleum Geologists Memoir 10*, p. 1–31.
- Nieuwenhuijzen, M. E., and van Steijn, H., 1990, Alpine debris flows and their sedimentary properties. A case study from the French Alps: *Permafrost and Periglacial Processes*, v. 1, p. 111–128.
- Okuda, S., Suwa, H., Okunishi, K., Yokoyama, K., and Nakano, M., 1980, Observations on the motion of a debris flow and its geomorphological effects: *Zeitschrift für Geomorphologie, supplement*, v. 35, p. 142–163.
- Okuda, S., Suwa, H., Okunishi, K., and Yokoyama, K., 1981, Depositional processes of debris flow at Kamikamihori fan, Northern Japan Alps: *Japanese Geomorphological Union, Transactions*, v. 2, p. 353–361.
- Pierson, T. C., 1980, Erosion and deposition by debris flows at Mt. Thomas, North Canterbury, New Zealand: *Earth Surface Processes*, v. 5, p. 227–247.
- Pierson, T. C., 1981, Dominant particle support mechanisms in debris flows at Mt. Thomas, New Zealand, and implications for flow mobility: *Sedimentology*, v. 28, p. 49–60.
- Pierson, T. C., 1984, Why debris flows stop: *Geological Society of America Abstracts with Programs*, v. 16, p. 623.
- Pierson, T. C., 1986, Flow behavior in channelized debris flows, Mount St. Helens, Washington, in Abrahams, A. D., ed., *Hillslope processes*: Boston, Allen and Unwin, p. 269–296.
- Punongbayan, R. S., Newhall, C. G., and Hoblitt, R. P., 1996, Photographic record of rapid geomorphic change at Mount Pinatubo, 1991–94, in Newhall, C. G., and Punongbayan, R. S., eds., *Fire and mud: Eruptions and lahars of Mount Pinatubo: Quezon City, Philippine Institute of Volcanology and Seismology, and Seattle, University of Washington Press*, p. 21–66.
- Rickmers, W. R., 1913, *The Duab of Turkestan*: Cambridge University Press, 563 p.
- Rodolfo, K. S., Arguden, A. T., Solidum, R. U., and Umbal, J. V., 1989, Anatomy and behavior of a post-eruptive rain lahar triggered by a typhoon on Mayon Volcano, Philippines: *International Association of Engineering Geology Bulletin*, v. 40, p. 55–66.
- Schiffman, R. L., Chen, A. T. F., and Jordan, J. C., 1969, An analysis of consolidation theories: *American Society of Civil Engineers Proceedings, Journal of the Soil Mechanics and Foundation Division, SM1*, p. 285–312.
- Schminke, H. U., 1967, Graded lahars in the type sections of the Ellensburg Formation, south-central Washington: *Journal of Sedimentary Petrology*, v. 37, p. 438–448.
- Schonfeld, B., 1996, Roll waves in granular flows and debris flows [Master's thesis]: Montreal, Canada, McGill University, 160 p.
- Schwab, W. C., Lee, H. J., Twichell, D. C., Locat, J., Nelson, C. H., McArthur, W. G., and Kenyon, N. H., 1996, Sediment mass-flow processes on a depositional lobe, outer Mississippi Fan: *Journal of Sedimentary Research*, v. 66, p. 916–927.
- Scott, K. M., 1988, Origins, behavior, and sedimentology of lahars and lahar-runout flows in the Toutle-Cowlitz River system: U.S. Geological Survey Professional Paper 1447-A, 76 p.
- Sharp, R. P., and Nobles, L. H., 1953, Mudflow of 1941 at Wrightwood, southern California: *Geological Society of America Bulletin*, v. 64, p. 547–560.
- Singewald, J. T., 1928, Mudflow as a geologic agent in semiarid mountains: *Comment: Geological Society of America Bulletin*, v. 39, p. 480–483.
- Suwa, H., 1988, Focusing mechanism of large boulders to a debris-flow front: *Japanese Geomorphological Union Transactions*, v. 9, p. 151–178.
- Suwa, H., and Okuda, S., 1983, Deposition of debris flows on a fan surface, Mt. Yakedake, Japan: *Zeitschrift für Geomorphologie, supplement*, v. 46, p. 79–101.
- Takahashi, T., 1978, Mechanical aspects of debris flow: *American Society of Civil Engineers Proceedings, Journal of the Hydraulics Division*, v. 104, p. 1153–1169.
- Takahashi, T., 1991, Debris flow: Rotterdam, A. A. Balkema, 165 p.
- Tanner, L. H., and Hubert, J. F., 1991, Basalt breccias and conglomerates in the lower McCoy Brook Formation, Fundy Basin, Nova Scotia: Differentiation of talus and debris-flow deposits: *Journal of Sedimentary Petrology*, v. 61, p. 15–27.
- Terzaghi, K., 1923, Die Berechnung der Durchlässigkeitsziffer des Tones aus dem Verlauf der Hydrodynamischen Spannungsercheinungen: *Akademie der Wissenschaften in Wien, Sitzungsberichte: Mathematisch-Naturwissenschaftliche Klasse, part IIA*, v. 132, no. 3/4, p. 125–128.
- Terzaghi, K., 1943, *Theoretical soil mechanics*: New York, John Wiley and Sons, 510 p.
- Terzaghi, K., 1956, Varieties of submarine slope failures: *Proceedings of Eighth Texas Conference on Soil Mechanics and Foundation Engineering*: Austin, University of Texas, Bureau of Engineering Research, Special Publication 29, September 14–15, p. 3.1–3.41.
- Vallejo, L. E., 1979, An explanation for mudflows: *Geotechnique*, v. 29, p. 351–354.
- Wasson, R. J., 1978, A debris flow at Reshun, Pakistan Hindu Kush: *Geografiska Annaler*, v. 60, p. 151–159.
- Webb, R. H., Pringle, P. T., Reneau, S. L., and Rink, G. R., 1988, Monument Creek debris flow, 1984: Implications for formation of rapids on the Colorado River in Grand Canyon National Park: *Geology*, v. 16, p. 50–54.
- Whipple, K. X., and Dunne, T., 1992, The influence of debris-flow rheology on fan morphology, Owens Valley, California: *Geological Society of America Bulletin*, v. 104, p. 887–900.
- Yano, K., and Daido, A., 1965, Fundamental study on mud-flow: *Kyoto, Disaster Prevention Research Institute Bulletin*, v. 14, no. 2, p. 69–83.
- Yould, T. L., 1973, Liquefaction, flow, and associated ground failure: *U.S. Geological Survey Circular 688*, 12 p.

MANUSCRIPT RECEIVED BY THE SOCIETY MAY 11, 1998

MANUSCRIPT ACCEPTED DECEMBER 17, 1998